Joint Special Interest Group meeting between euspen and ASPE
Advancing Precision in Additive Manufacturing
KU Leuven, Belgium, September 2023
www.euspen.eu

Mould manufacturing by hybrid laser powder bed fusion of M789 steel on a functional base

J. Metelkova[1], U. Paggi[2], I. Marco[2], M. Sinico[1,3], L. Thijs[2], B. Van Hooreweder[1]

[1]*Department of Mechanical Engineering, KU Leuven, 3001 Leuven, Belgium*
[2]*3D Systems Leuven, 3001 Leuven, Belgium*
[3]*Flanders Make@KU Leuven, 3001 Leuven, Belgium*

brecht.vanhooreweder@kuleuven.be

Abstract
This research focuses on reducing the manufacturing cost of metal components through "hybrid additive manufacturing", i.e. laser powder bed fusion (LPBF) carried out on a pre-machined functional base. By incorporating part of the final component's geometry (such as cooling channels) in the base, the cost for large and bulky products can be minimized. The study identifies two crucial quality requirements for such a hybrid process: (1) reaching sufficient quality of the interface zone between the conventionally manufactured base and the LPBF part and (2) achieving accurate alignment between the base and the top LPBF section. A sensitivity study was performed using LPBF of M789 novel steel on a machined M303 steel base, demonstrating high-quality microstructural integrity even for a large misalignment in the building direction (Z). The alignment in the horizontal plane (XY) was carried out using calibration and process monitoring tools provided by 3D Systems, keeping the deviations <95 µm for real production simulated environments. Finally, the alignment procedure was successfully applied to a mould demonstrator, confirming an average channel misalignment of 49 µm.

Alignment, Hybrid Manufacturing, Laser Powder Bed Fusion, Mould

1. Introduction

Laser powder bed fusion (LPBF) is a metal additive manufacturing (AM) method which is widely reported in scientific literature [1] and its industrial applications are as well progressively increasing [2]. In LPBF the part is built layer by layer, by depositing a fine layer of metal powder and its selective laser scanning following the component's cross-section. The low layer thickness (typically 30-100 µm) allows producing intricate shapes, optimized cooling channels or lightweight structures. However, the cost to manufacture industrial components (e.g. moulds) entirely by LPBF remains often higher compared to conventional subtractive manufacturing techniques. In fact, moulds typically contain bulkier sections which are not very well suited for the LPBF process as: (1) large sections require a long scanning time, significantly increasing the production time and cost, and (2) they are more prone to quality issues.

This work presents a "hybrid" AM technology combining subsequently both conventional and additive approaches. It solves the two above mentioned shortcomings, while enabling manufacturing designs otherwise impossible to produce conventionally. This method consists in additive building of smaller components on top of a bulky conventionally manufactured base with a flat top surface. The final product will comprise both the LPBF section and the base. The base becomes hence functional, including final component's geometry, e.g. straight milled cooling channels on top of which intricate, highly performant topology-optimized cooling channels and other complex features of the mould can be additively built [3].

The main challenge of such a hybrid AM technique concerns an accurate alignment between the conventional base and the LPBF part built on top. The vertical (Z) alignment not only affects the final component's dimensions, but also directly impacts the quality of the interface zone, which is highly material-specific. LPBF on a functional base plate has already been reported, focusing on the interface zone quality [3–5]. In the standard LPBF process, a misalignment in the horizontal plane (XY) up to several millimetres between the nominal and actual part position can be accepted. However, this is insufficient for hybrid AM. Some studies reported alignment methods for hybrid LPBF in Z axis [6] and XY plane [7,8]. However, the presented methods are either time consuming [7] or inaccurate [8]. A swift, repeatable and accurate XY alignment method would be hence beneficial. The purpose of the approach presented here is to provide a solution applicable to a commercial LPBF machine with a photodiode-based monitoring system. Currently, 3D Systems is developing a new tool [9] by using their DMP monitoring sensing capabilities [10–12]. This tool aims to accurately locate the position of the preform (within 100 µm from the desired position) by using referencing features, photodiode signal variation and link the LPBF machine coordinate system.

The first part of this paper focuses on the repeatability of the first deposited powder layer and on material's sensitivity to metallurgical defects resulting from a typical misalignment in Z. The investigated material is a novel maraging steel M789 reported earlier in [13,14]. M789 was built by LPBF on a conventionally manufactured steel base from M303, typically used in tooling industry. In the next step, the XY alignment tool and methodology developed by 3D Systems are investigated. This includes repeatability and accuracy of the feature detection method, application to the real machine conditions and the effect of the manual base positioning by the operator. Finally, two mould demonstrators are built and their misalignment is quantified by a coordinate measurement machine (CMM).

2. Experimental setup

The experiments were carried out in a ProX® DMP 320B metal printer (LPBF machine) from 3D Systems. The selected powder

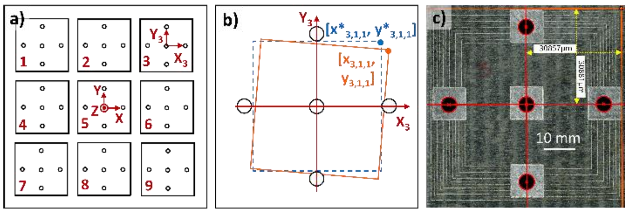

Figure 1. (a) Illustration of the test plate with numbers referring to the test locations *i*, (b) detail of a test location with one calibration square, (c) example of a measurement.

was AMPO M789 tool steel powder manufactured by Böhler, with a particle size distribution $d_{10\text{-}90}$≈20-50 µm [15]. The LPBF process was done using the *Certified M789* process parameters for layer thickness of 60 µm released by 3D Systems. The base plate was made from M303 steel [16], which is a standard material for industrial mould applications. The base plate had dimensions of 272 mm x 272 mm and thickness >10 mm. In the machine coordinate system, the XY (horizontal) plane is perpendicular to the LPBF building direction (BD) or Z axis.

2.1. Z axis alignment and measurement procedure

To start, an operator-sensitivity study for the first layer deposition was carried out. In LPBF machines, contrary to conventional manufacturing methods, the relative zero (Z=0) does not correspond to a specific absolute machine coordinate but refers to the relative height difference between the powder coating blade and the top of the base plate. As a matter of fact, Z=0 is typically determined visually by depositing a fine layer of powder on the levelled base plate and moving the build cylinder up until no powder remains on the plate. The goal of this first step is to quantify the effect of the operator on the thickness of the first deposited powder layer. This is done by recording the variation in absolute machine coordinates *ΔZ* after base plate alignment by four trained operators. A total of two base plates were aligned each four times.

In a second step, a material sensitivity study was performed by building 7 mm x 7 mm x 5 mm blocks from M789 on the M303 base plate. The first layer height *ΔLT* varied from 60 µm to 240 µm from the previously established relative zero. Two strategies for the first layer scanning were investigated, a "standard" and "remelting" scanning strategy, referring to layer scanning once or twice, respectively.

2.2. XY-plane alignment and measurement procedure

The alignment in the XY plane ("calibration") was performed using the calibration and DMP monitoring tools provided by 3D Systems. The method is based on photodiode signals from two off-axis sensors [10–12]. As illustrated in Fig. 1, a set of reference features (here Ø5 mm alignment holes with a sharp edge) is scanned with the laser, the contour of each hole is detected and its centre located [9]. An average location based on the two sensors is then calculated. After comparing the nominal and detected location of the set of reference features, a translation offset in X and Y direction as well as a rotation offset around the Z axis is applied to the LPBF component. This procedure is referred to as "calibration run".

As summarized in Table 1, the calibration method was investigated under three test conditions (TC) specified below. After each calibration run, a simple validation feature (single-line square) is scanned. Then the misalignment of each of its corners with respect to a reference position is assessed, expressed as misalignment in X (*ΔX*), Y (*ΔY*) and the total misalignment (*ΔXY*). For each TC the maximal and the average misalignment (ΔXY_{max} *and* ΔXY_{avg}) is given, as well as its 68 % confidence interval CI (corresponding to one standard deviation σ). As illustrated in Fig. 1, the base plate is divided into 9 test locations ("mini-plates"), each containing five Ø5 mm reference holes (one central hole and four holes distanced 25 mm from the centre). Each TC was applied to all mentioned test locations.

After investigating the calibration accuracy and repeatability, two mould demonstrator parts were manufactured, each containing four Ø5 mm reference holes, distanced 7 mm from the centre point. LPBF cooling channels were built on top of these reference holes and the misalignment between the machined and LPBF channels was evaluated with a CMM machine (3D CMM Mitutoyo FN905H with a maximum permissible error of 4.2 µm + 5 µm/m).

<u>TC1: Repeatability of the reference feature detection</u>

The calibration run is performed five times and the translation and rotation offset given by the calibration software is applied to a 50 mm square validation feature. For each corner, the misalignment from the average corner location is calculated.

<u>TC2: Misalignment of the calibrated validation features</u>

Following each calibration run, a square with side lengths of 40-62 mm is scanned and the misalignment of its corners with respect to the intended position is measured with an optical microscope (Keyence VHX-6000). The objective of this test is to measure the misalignment under real machine conditions. As illustrated in Fig. 1b,c, on each test location a local X_iY_i coordinate system can be determined, the axes defined as a best fit between the centres of three reference holes. The misalignment $\Delta XY_{i,j,k}$ of each of the four corners of the square is defined in Eqs. (1-3) with $\Delta X_{i,j,k}$ and $\Delta Y_{i,j,k}$ misalignment in x and y direction, respectively, $x^*_{i,j,k}$ and $y^*_{i,j,k}$ nominal corner coordinates (20 mm < $|x^*_{i,j,k}|$ < 31 mm, $|x^*_{i,j,k}|=|y^*_{i,j,k}|$) and $x_{i,j,k}$ and $y_{i,j,k}$ measured coordinates of a corner point *k* of square *j* on test location *i* (Fig. 1c).

$$\Delta X_{i,j,k} = x_{i,j,k} - x^*_{i,j,k} \tag{1}$$

$$\Delta Y_{i,j,k} = y_{i,j,k} - y^*_{i,j,k} \tag{2}$$

$$\Delta XY_{i,j,k} = \sqrt{\Delta X^2_{i,j,k} + \Delta Y^2_{i,j,k}} \tag{3}$$

<u>TC3: Misalignment of the calibrated validation features after repeated base plate re-positioning</u>

The last test condition is identical to TC2, except for a manual base plate re-positioning between each calibration run. Thus, it includes also the effect of the operator on the misalignment. The test was not performed on a single base plate, but on 9 separate mini-plates attached to the large base plate by four screws each.

3. Results and discussion

3.1. Effect of the operator in Z axis alignment

As the initial step in this study, the effect of the operator on determining the relative zero powder layer (Z=0) was

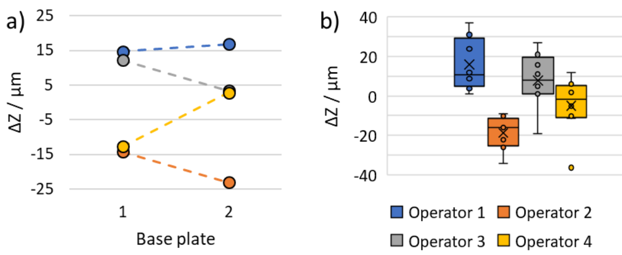

Figure 2. Effect of the operator for determining the relative zero, (a) average for four repetitions, (b) overview of the total spread.

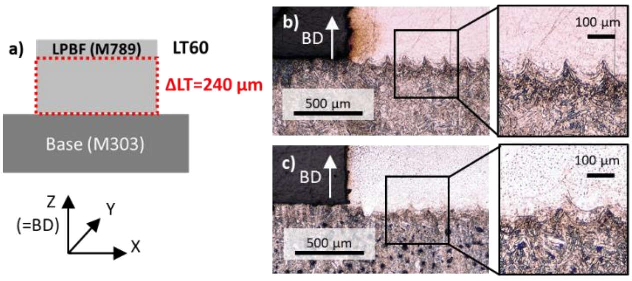

Figure 3. (a) Illustration of the varied first layer deposition height; metallurgical cross-section of samples with ΔZ=240 µm, (b) standard process parameters and (c) remelting strategy for the first LPBF layer.

investigated, referring to the alignment of the recoater blade with respect to the base plate. As shown in Fig. 2, if the Z alignment carried out by a trained operator was repeated multiple times, the misalignment $|\Delta Z|$ can be estimated within 23 µm. In case of a single alignment, $|\Delta Z|$ ranges up to 37 µm, a value comparable to a typical layer thickness used in LPBF.

3.2. Material sensitivity to the first layer deposition height

Fig. 3 shows vertical cross-sections of the hybrid samples with a purposely increased height of the first deposited layer by ΔLT=60-240 µm from the previously established Z=0. The difference in microstructure between the base material (M303) and the printed part (M789) leads to a different etching behaviour which facilitates the discrimination of both sections. Furthermore indications of the shape and size of the first layer melt pools can be estimated. Note that the difference in etching behaviour also made it difficult to get a gentle etch for both parts leading to overetching artefacts as, for example, in the base material section in Fig. 3c. Evaluation of the as-polished cross-sections confirmed that the black dots in the base are due to overetching and not due to porosity.

The process window for the combination of printing M789 with LPBF on top of M303 base material seems to be very wide. For both the standard and remelting scanning strategies, the interface between the base and the LPBF part appears to be fully dense with no indications of lack of melting nor other porosities.

As discussed above, there is a significant difference in microstructure between the base material and the printed material. This transition zone is rather small in the order of magnitude of 100 µm and follows a staggered interface due to the nature of the melt pool shape. The melt pools at the interface look stable and in conduction melting mode. Furthermore, no signs of instabilities were observed for 5 mm or for 120 µm high parts, nor for larger cross sections (60 mm x 60 mm). Considering these observations, the misalignment ΔZ of the first deposited layer height (see Section 3.1) still appears to be well within the process window limits of the scanning parameters for the first layer.

3.3. Accuracy of the XY-plane alignment of the LPBF part

The investigation of the XY plane alignment (calibration) started with a repeatability study of the feature detection method (TC1). TC1 included five identical calibration runs at each test location, and the calculated offset was applied to a square validation feature. As given in Fig. 4a and Table 1, the average calculated misalignment ΔXY_{avg} is 8.8 µm ± 6.3 µm (referring to 68 % confidence interval CI), with a maximal misalignment ΔXY_{max}=28.5 µm. However, it is noteworthy that the middle test location (i=5) showed a significantly lower variability (ΔXY_{avg}=2.7 µm ± 1.6 µm) compared to the other test locations (ΔXY_{avg}=9.5 µm ± 6.3 µm). A certain variation between the center and the edges of the base plate is to be expected, considering the laser-based alignment approach. In summary, ΔXY_{avg} can be estimated with 95 % CI <21.4 µm.

Following the analysis of the outcome of the calibration software (TC1), the second test (TC2) involved actual scanned calibrated features. TC2 included analysis of measured misalignment of the square validation features with respect to the coordinate system given by the reference holes (Fig. 1c). As shown in Fig. 4b and Table 1, ΔXY_{avg} increased by a factor of 5 compared to TC1 (ΔXY_{avg}=45.8 µm± 24.5 µm, ΔXY_{max}=110.5 µm). As a matter of fact, in addition to the sources of misalignment for TC1, TC2 is performed in real machine conditions. This includes possible melt pool instabilities leading to a slight wobbling (lowering the line scan straightens), melt pool asymmetricity due to the laser incidence angle on the given test

Table 1 Overview of the test campaign, with the average and maximal misalignment ΔXY_{avg} and ΔXY_{max}, respectively. CI referes to confidence interval.

	TC1 **Reference feature detection**	**TC2** **Measured misalignment**	**TC3** **Effect of the operator**	**Validation** **(demonstrator part)**
Number of test locations	9	9	9	2
Number of calibration runs	5	5	3	1
Total number of data points	180 (=9 · 5 · 4)	180 (=9 · 5 · 4)	108 (=9 · 3 · 4)	8 (=2 · 1 · 4)
Manual re-positionning	no	no	yes	no
Assessed validation feature	square line scan	square line scan	square line scan	channel alignment
Assessment method	calculated	measured (optical)	measured (optical)	measured (CMM)
$\Delta XY_{avg} \pm \sigma$ / µm (=68 % CI)	8.8 ± 6.3	45.8 ± 24.5	44.0 ± 24.5	48.5 ± 20.1
$\Delta XY_{avg} + 2\cdot\sigma$ / µm (=95 % CI)	21.4	94.8	93.0	88.7
ΔXY_{max} / µm	28.5	110.5	111.8	77.0

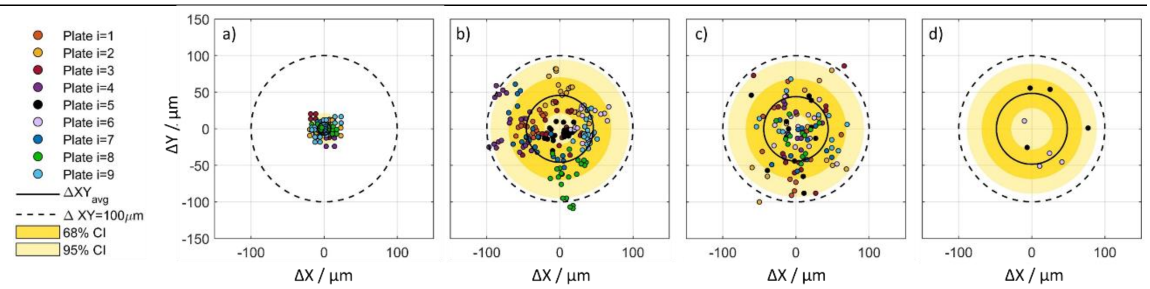

Figure 4. Misalignment ΔX and ΔY based on (a) the calibration software outcome (TC1) and measured misalignment by optical microscopy (b) without (TC2) or (c) with (TC3) the additional manual re-positioning by an operator, and (d) misalignment on the demonstrator part measured by CMM.

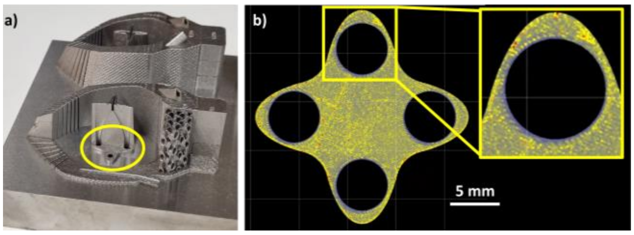

Figure 5. Validation mould Demonstrator. (a) photo showing the aligned holes, (b) photodiode signal from the first layer of the aligned holes.

location, or the error originating from the focal plane calibration. Among others also for these reasons a lower variability was observed for the middle test location (i=5, ΔXY_{avg}=15.0 µm ± 6.1 µm) compared to the other ones (ΔXY_{avg}=49.6 µm ± 21.7 µm). Moreover, the actual measurement error should be also taken into account. The repeatability of the measurement method was assessed by repeating the measurement of a square five times, resulting in a typical 95 % CI deviation (2σ) for ΔX or ΔY of ≈10 µm. Furthermore, the manufacturing precision of the reference features also plays a role in determining ΔXY for TC2. In the investigated setup the average distance from the central hole of the mini-plate measured with a CMM machine was 24.996 mm ± 44 µm (95 % CI) compared to the nominal 25 mm. Although the relative position of the holes was reasonably accurate, the absolute coordinates were located up to 600 µm from the nominal position. In the end, despite all these sources of misalignment, most of the measured points after calibration remained within the desired ΔXY=100 µm ($\Delta XY_{avg}+2\cdot\sigma$=94.8 µm). On some test locations, TC2 was also performed using the measured CMM coordinates instead of the nominal coordinates. However, no significant effect on ΔXY was observed, and for the sake of simplicity using nominal coordinates is a preferred solution.

In the last step, the effect of the operator was investigated (TC3), by manual mini-plate repositioning between each calibration run. As shown in Fig. 4c and Table 1, this does not seem to affect the misalignment compared to TC2 (ΔXY_{avg}=44.0 µm ± 24.5 µm, ΔXY_{max}=111.8 µm). It hence confirms the efficiency of the calibration software tool.

3.4. Validation via a mould demonstrator part

As discussed in Section 3.3, using a single line scan feature involves drawbacks such as melt pool wobbling or assymetricity with respect to its middle line. In order to validate the reported results, two full mould demonstrator components (Fig. 5a) were manufactured. Each part contained four reference holes, on top of which cooling channels were built by LPBF (Fig. 5b). Fig. 4d and Table 1 show the misalignment between the drilled and LPBF holes measured with CMM (ΔXY_{avg}=48.5 µm ± 20.1 µm, ΔXY_{max}=*70 µm*). Fig. 5b shows the photodiode signal from the first LPBF layer, with overhanging zones displayed in blue. Their symmetricity indicates a good level of alignment, confirming the results from Fig. 4d.

Considering the typical industrial machining oversize of 100-500 µm, this level of accuracy appears to be suitable for real industrial applications. Moreover, the setup time for this procedure is also industrially acceptable: 9 calibration runs took <3 min, corresponding to scanning and analyzing five reference holes at each location in ≈18 sec. If the reference features are machined cooling channels, such as in the case of the demonstrator part described above (Fig. 5a), no additional manufacturing time is needed.

4. Conclusions

In this paper a new alignment approach for hybrid additive manufacturing is investigated, referring to performing laser powder bed fusion (LPBF) on a functional base plate which will eventually become part of the final product. The two main requirements were addressed, focusing (1) on the quality of the interface zone and (2) on the alignment accuracy between the base plate and LPBF section.

- The repeatability of the alignment in the building direction (Z) carried out by a trained operator was observed within one typical layer thickness (37 µm).
- Thanks to the broad processing window, the material combination of M303 base plate and M789 built by LPBF shows high-quality microstructural integrity without any visible defects even for a large misalignment in the building direction (240 µm).
- The XY calibration procedure for horizontal alignment developed by 3D Systems shows promising results within the typical industrial requirements. The accuracy of the feature detection method is high (average misalignment <10 µm). Based on the misalignment measurements of 72 single line scan features, the proposed procedure leads to an alignment accuracy within 95 µm (with a 95 % confidence interval). Several outliers were observed as well, ranging up to 112 µm. Furthermore, the calibration accuracy was confirmed by CMM measurements on a fully built mould demonstrators, leading to an average misalignment of 49 µm.

In summary, the proposed method appears to be an accurate method suitable for reducing manufacturing or repair cost of industrial components with bulky and finer sections.

Acknowledgements

This research was funded by VLAIO, Grant Agreement No. HBC.2020.2958 (SIM-ICON project METAMOULD).

References

[1] DebRoy T et al. 2018 *Prog Mater Sci.* 92:112–224.
[2] Vafadar A et al. 2021 *Appl Sci*. 11(3):1213.
[3] Popov VV, Fleisher A. 2020 *Manuf Rev*. 7:6.
[4] Kučerová L et al. 2020 *Addit Manuf*. 32:101108.
[5] Shakerin S et al. 2019 *Addit Manuf*. 29:100797.
[6] Wilm J et al. 2021. Computer vision based zero point estimation for hybrid builds in metal additive manufacturing. *Proc aspe-euspen.*
[7] Merz B et al. 2023 *Int J Adv Manuf Technol*. 125(5):2409–24.
[8] Kulkarni P et al. In: Reddy ANR et al, editors. Singapore: Springer; 2020. p.221–9., doi.org/10.1007/978-981-15-1616-0_21.
[9] Coeck S, Van Vaerenbergh J. 2021. System for Aligning Laser System to a Carrier Plate. EP3736111B1.
[10] Bisht M et al. 2018 *Addit Manuf*. 22:302–6.
[11] Ray N et al. 2018. *Proc SFF*.
[12] Coeck S et al. 2019 *Addit Manuf*. 2019 25:347–56.
[13] Turk C et al. 2019 *BHM*. 164(3):112–6.
[14] Sinico M et al. 2022 *Proc CIRP*. 111:162–5.
[15] M789 AMPO - BÖHLER Edelstahl GmbH & Co KG [Internet]. [cited 2023 Jun 15]. Available from: https://www.bohler-edelstahl.com/en/products/m789-ampo/
[16] M303 - BÖHLER Edelstahl GmbH & Co KG [Internet]. [cited 2023 Jun 15]. Available from: https://www.bohler-edelstahl.com/en/products/m303/